https://doi.org/10.1016/j.mechmat.2020.103316

# NEUTRON STRAIN SCANNING FOR EXPERIMENTAL VALIDATION OF THE ARTIFICIAL INTELLIGENCE BASED EIGENSTRAIN CONTOUR METHOD

Fatih Uzun[a,1], Chrysanthi Papadaki[a], Zifan Wang[a], Alexander M. Korsunsky[a,2]

[a]MBLEM, University of Oxford, Department of Engineering Science, Oxford, U.K.

[1]fatihuzun@me.com, fatih.uzun@eng.ox.ac.uk

[2]Corresponding Author, alexander.korsunsky@eng.ox.ac.uk

Authors' Accepted Manuscript

Published version in *Mechanics of Materials*

Volume 143, 2020, 103316

https://doi.org/10.1016/j.mechmat.2020.103316

**ABSTRACT**

The demand on energy generation with low carbon emissions evoked the development of ultra-super critical technology that allows operating steam turbines at high temperature and pressure conditions. However, operating at extreme conditions necessitates careful considerations on structural integrity which is affected by residual stresses. Welding is used for joining of components of steam turbines, but this process causes formation of residual stresses at very complex forms as a result of this process. Careful investigations are necessary to understand distribution of harmful residual stress fields. The eigenstrain theory was previously used for the development of the artificial intelligence based eigenstrain (AI-eig) contour method that allowed advanced modelling of the behaviour of Inconel alloy 740H under thermo-mechanical loading conditions. The models created based on this method are capable of determining the residual stress fields in the whole specimen or in the parts and slices created using electric discharge machining (EDM). In the previous applications of the AI-eig contour method, the determination of the distribution of eigenstrain fields in as-welded and heat-treated specimens was followed by the calculation of volumetric residual stresses. In this study, long- and short-transverse components of the residual strains determined by the AI-eig contour method applied to EDM-cut surfaces of the parts of as-welded and heat-treated specimens were validated using the neutron strain scanning method. The results demonstrate the effectiveness of the integrative modelling approach that enables the determination of eigenstrains in the whole specimen and the calculation of residual strains before and after the machining process.

**Keywords:** Neutron strain scanning; Residual strain; Artificial intelligence; Eigenstrain contour method; Reconstruction; Inconel alloys

https://doi.org/10.1016/j.mechmat.2020.103316

## 1. INTRODUCTION

In spite of the fact that renewable sources has an increasing demand on energy generation, the amount of greenhouse gases released to the atmosphere continues to increase (Blunden and Arndt, 2019), because of the increasing consumption of fossil fuels in the world (Ritchie and Roser, 2019). According to U.S. Energy Information Agency, 37 % of world energy production will still be performed by burning coal (U.S. Energy Information Agency, 2013). Advanced ultra-supercritical technology promises to reduce carbon emissions of power plants that use fossil fuels by increasing the efficiency of steam turbines (Gianfrancesco, 2017). The use of high strength superalloys with creep resistance allows operating steam turbines at high temperature and pressure conditions, but structural integrity of their components is affected negatively in the case of availability of residual stress that are formed at high magnitudes during the welding of components of steam turbines. Accordingly, investigation of the sources of residual stresses is crucial to have high quality designs with improved safety and long service life.

The inverse eigenstrain method has been advanced over the last two decades as a powerful general and uniform approach to the numerical evaluation of complex residual stress fields. Fundamentally, the use of eigenstrain basis for residual stress and strain matching ensures the satisfaction of core mechanics requirements: stress equilibrium and strain compatibility in the bulk of the sample, and boundary conditions (Korsunsky, 2017). This approach regularises the inverse problem in comparison e.g. with simply trying to match stresses (even ensuring zero balance of force and moment); and underlies the predictive power and reliability of the eigenstrain reconstruction method.

https://doi.org/10.1016/j.mechmat.2020.103316

After elucidating the eigenstrain sources of the welding residual stress (Uzun and Korsunsky, 2018), the principles of artificial intelligence were combined with eigenstrain theory (Uzun and Korsunsky, 2019a) for accurate modelling of complex processes with high accuracy and reduced computational cost. Artificial intelligence based eigenstrain contour method allows the determination of eigenstrain fields and calculation of volumetric residual stresses within large scale welded components and simulation of creep mechanism (Uzun and Korsunsky, 2019b). The bead-on-plate design created complex thermo-mechanical loading conditions that necessitated the determination of eigenstrain distribution in three principal axes, going beyond the determination of planar distribution of eigenstrain based on the assumption that the weld is "continuously processed" (DeWald and Hill, 2006; Kartal et al., 2016), i.e. uniform in the longitudinal z-direction of the weld.

In addition to the complex nature of the bead-on-plate weld design, the artificial intelligence based eigenstrain contour method necessitates the modelling of the whole welded specimen and the machined EDM-cut state of the same specimen. Because this model aims to minimize the mean squared error between measured and calculated out-of-plane displacements appeared as a result of cutting process. Modelling of EDM-cut state is done based on the theoretical assumption that distribution and magnitude of permanent plastic strains does not change after the cutting process.

Neutron diffraction validation of the contour method (Brown et al., 2011; Kartal et al., 2006; Kelleher et al., 2003; Rangaswamy et al., 2005; Woo et al., 2013; Zhang et al., 2003) was reported previously, but this highly advanced experimental technique has not been used for the validation of the eigenstrain contour methods. The artificial intelligence based eigenstrain contour method has been used to reconstruct all principal components of residual strains using

https://doi.org/10.1016/j.mechmat.2020.103316

a limited set of experimental data corresponding to only one or two principal components. This property of the AI-eig contour method has been used for the reconstruction of the residual strains in Inconel alloy 740H, that are normal to the direction of experimentally determined out-of-plane displacements, before and after the EDM cut process. In this study, the capability of AI-eig eigenstrain contour method on reconstruction of residual strains after a chain of processes from welding to cutting using only a single component of experimental data is represented by validating the calculations of the AI-eig eigenstrain contour method corresponding to the after-cut state using the neutron strain scanning measurements after the cutting process.

## 2. BEAD-ON-PLATE WELDMENTS

Inconel alloy 740H was designed by Special Metals Corporation Company in order to fulfil requirements of ultra-super critical technology used for coal-fired boilers and steam turbines. This nickel-based superalloy has high strength and creep resistance at high temperature and pressure conditions. In this study, two identical specimens of Inconel alloy 740H were prepared according to the design illustrated in Figure 1. Origin of the three-dimensional coordinate system is located at the bottom of the centre of the rectangular plate where Planes A and B intersect. The bead-on-plate design has a weld slot that expands along one third of the length of the specimen with a depth of 5 mm. After machining of the materials, the plates with weld slots were annealed at 1107 ºC for 1 hour and water cooled to obtain a stress-free state. Weld slots of the annealed specimens were filled with 3-pass weld beads using tungsten inert gas (TIG) technique using the parameters given in Table 1.

https://doi.org/10.1016/j.mechmat.2020.103316

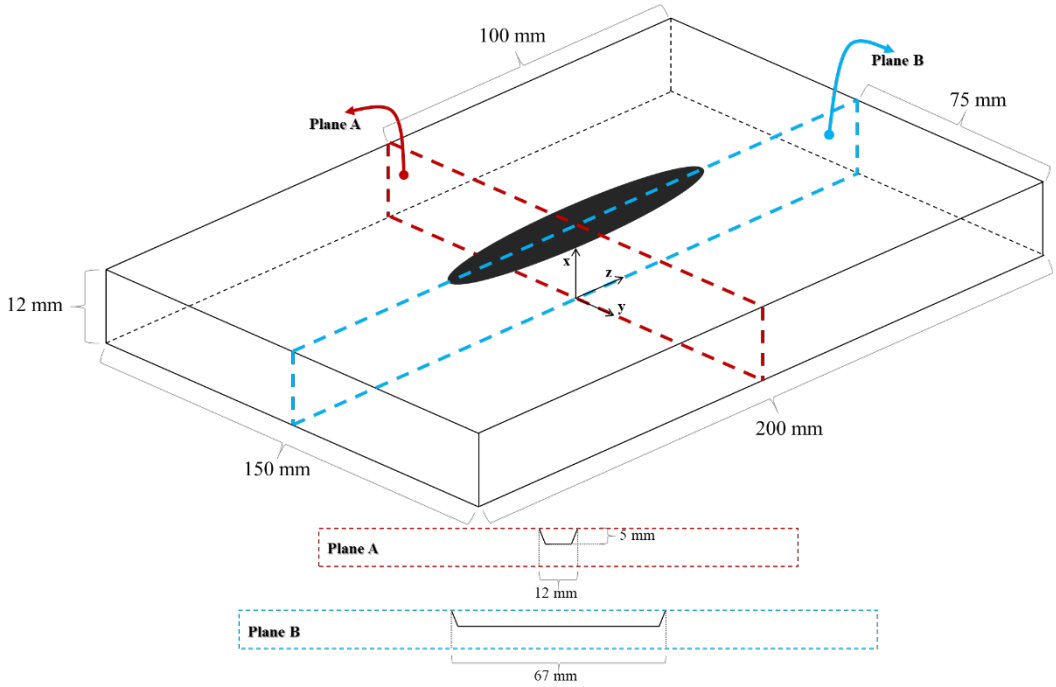


Figure 1. Three-dimensional representation of bead-on-plate weldment geometry (Uzun and Korsunsky, 2019a, 2018).

One of the specimens was left as-welded and the other specimen was post-weld heat treated (aged) at 800 ºC for 4 hours and air cooled in order to investigate stress relaxation as a result of aging process. Parameters of annealing and aging processes are determined by the manufacturer according to their product specifications, so that no further investigations related to these parameters were done during this study. Chemical composition of the alloy was composed of chromium, 24.5%, cobalt, 20.0%, aluminium, 1.35%, titanium, 1.35%, and niobium, 1.5%, with nickel balance. Iron, carbon, manganese, molybdenum, silicon, copper, phosphorus, sulphur and boron elements were included at nominal ratios. The filler material of the weld had the same chemical composition with the base plates. Both as-welded and heat-treated specimens were cut from Plane A using EDM technique and contour measurements were performed on each surface of both cut planes. The contour data from each surface were averaged and processed for being used in the determination of eigenstrain fields.

https://doi.org/10.1016/j.mechmat.2020.103316

Table 1. Parameters of manual TIG welding process

| | Weld Pass 1 | | Weld Pass 2 | | Weld Pass 3 | |
|---|---|---|---|---|---|---|
| | AW | HT | AW | HT | AW | HT |
| Current (A) | 174.0 | 174.0 | 174.0 | 174.0 | 174.0 | 174.0 |
| Voltage (V) | 16.1 | 16.0 | 16.3 | 16.5 | 16.3 | 16.2 |
| Travel Speed (mm/min) | 163.0 | 136.4 | 152.4 | 111.5 | 134.3 | 123.4 |
| Wire Speed (mm/min) | 177.8 | 254.0 | 228.6 | 304.8 | 177.8 | 228.6 |
| Shielding Gas (Ar.He) | 75/25 | 75/25 | 75/25 | 75/25 | 75/25 | 75/25 |
| Flow Rate (cfh) | 35 | 35 | 35 | 35 | 35 | 35 |

## 3. THE AI-EIG CONTOUR METHOD

Determination of all six components of residual stress using current measurement methods like FIB-DIC (Everaerts et al., 2018), contour (Prime et al., 2001), ultrasonic correlation (Uzun and Bilge, 2015) and diffraction (Smith et al., 2018) is impossible (Ahn et al., 2017). In order to deal with this problem, thermal-structural elastic-plastic models are used to determine residual stress fields and experimental methods function as validation tools that represent some of the principal components of residual stress. In the case of weld modelling, complexity increases because of the requirement of the determination of heat source geometry and temperature dependent material properties. Eigenstrain methods for the determination of volumetric residual stresses in weldments were developed as an alternative to classical weld modelling (DeWald and Hill, 2006; Uzun and Korsunsky, 2018). These methods converted elastic-plastic solution procedure with high computational demand into calculation of elastic strains using only the elastic properties of the material. The use of experimental data for the reconstruction process allows obtaining realistic results for all components of residual stress. This form of reconstruction process with low number of model variables allowed application

of principles of artificial intelligence for the purpose of leaving the decision-making steps of the solution procedure to an artificial agent.

The eigenstrain contour method (Uzun and Korsunsky, 2018) was previously combined with an artificial agent to develop artificial intelligence based eigenstrain contour method (Uzun and Korsunsky, 2019a, 2019b). Main property of the eigenstrain contour method is the determination of the distribution of eigenstrains, permanent plastic strains that cause formation of residual stresses, using linear combination of separate solutions of approximate polynomial functions. This process was implemented into a finite element model for solving linear elastic deformations. Among three different solution processes, multi-component iterative solution process of the eigenstrain contour method provided highest degree of match with experimental data (Uzun and Korsunsky, 2018) and this procedure allowed determination of weld distortions (Uzun et al., 2018). The AI-eig contour method eliminated the need for time consuming trial and errors, that increases the computation and labour cost drastically, for the determination of model variables by the model designer and continuous iteration processes. Details of the eigenstrain contour method, solution processes and combination of the eigenstrain contour method with the principles of artificial intelligence can be found in the papers mentioned in this paragraph.

Pre-mentioned eigenstrain models are able to perform solutions using different components of experimental data. Apart from being sensitive to the components of the experimental data, calculations on all components of deformations should be in correspondence with the available component of experimental data and this necessitates the validation of all components of calculated deformations. In the solution for determination of residual stresses in as-welded and heat-treated specimens of Inconel alloy 740H, single component of

experimental data which is parallel to the longitudinal z-component of residual strains was used and finite element solution provided all six components of residual stress. In this study, short transverse x- and long transverse y-component of residual strains, calculated by the artificial intelligence based eigenstrain contour method, were compared with the neutron strain scanning measurements.

Details of the solution procedure and optimum coefficients of the deterministic eigenstrain model were given in the pre-mentioned study of the present authors (Uzun and Korsunsky, 2019a). Four coefficients determine size and location of the plastic strain zone, where eigenstrains are located, two coefficients belong to the knee function, that determines the shape of the plastic strain zone in the longitudinal z-direction, and two coefficients determine fixed weight of the long transverse y- and longitudinal z-components of eigenstrains. The weight of two eigenstrain components, that provide closest match between displacements from model calculations and experimental measurements, were determined by the artificial agent based on the magnitude of eigenstrains calculated by the eigenstrain-contour method. For the details of the solution procedure that explains where the eigenstrain-contour method with deterministic finite element model is located in the artificial intelligence based model, readers should see flowchart given in pre-mentioned paper of the present authors (Uzun and Korsunsky, 2019a). The artificial agent uses evolutionary algorithms and after 60 generations the ratio between the long transverse y- and longitudinal z-components of eigenstrains was calculated to be 3.3345. All model coefficients are rational, and they are determined for each problem specifically. On the other hand, higher number of generations have a potential to provide improvements in the match between experimental data and model calculations, but it was observed that improvements after 30 generations were subsidiary.

https://doi.org/10.1016/j.mechmat.2020.103316

## 4. NEUTRON STRAIN SCANNING

Neutron diffraction is defined as a crystallographic method used to determine the atomic and/or magnetic structure of materials (Pang, 2014). Neutron radiation is able to penetrate depths at about 50 mm in engineering materials that is much higher than the penetration depth of X-Rays (Shokrieh and Ghanei Mohammadi, 2014). However, this technique has limited resolution and cannot measure residual strains within distances less than 1 mm (Prime, 1999) and neutron sources are characterized by relatively low fluxes compared to X-Ray sources in synchrotrons, and therefore the collecting time for each data point can be long.

The neutron strain scanning technique has been used for the determination of strains in materials since 1985 (Allen et al., 1985). One of the main advantages of this technique is that it allows a non-destructive analysis of the stress field in bulk samples. By applying Bragg's law, the inter-planar spacing ($d$) of the crystal lattice is evaluated and then used as an intrinsic strain gauge: strain is estimated by comparing the spacing of a stressed sample with that of an unstressed one. The strain is measured in the direction of the scattering vector, $Q = k_f - k_i$, which bisects the angle between incident and diffracted beams and is perpendicular to the diffracting crystallographic plane.

As a result of increasing demand on strain measurement for industrial and academic purposes, ENGIN (Johnson et al., 1997) was built at the pulsed neutron source ISIS as a neutron diffractometer the capability of high precision atomic lattice spacing measurement. ENGIN was upgraded to ENGIN-X (Santisteban et al., 2006) which provides performance improvement and allows measurement of the strain along any particular direction by rotating the sample as it was in ENGIN diffractometer (Allen et al., 1985). The beamline of ENGIN-X

https://doi.org/10.1016/j.mechmat.2020.103316

is optimised for strain measurements of crystalline materials using the atomic lattice planes and operates at a wavelength range from 0.5 $\dot{A}$ to 0.6 $\dot{A}$. The accurate measurement of polycrystalline lattice parameters allows the use of the atomic lattice planes as an atomic 'strain gauge'. In this study, time-of-flight diffraction experiments were performed on the ENGIN-X neutron diffractometer, ISIS, UK [2].

Neutron strain scanning of Inconel alloy 740H weldments were performed to define the macroscopic elastic strain tensor within the bulk of a gauge volume of 2×2×4 mm in order to capture most important features of strain field. The incident pulsed beam of neutrons entered to the plate with 45$^{o}$ angle to the plate surface and diffracted into the detectors at a 90$^{o}$ angle as illustrated in Figure 2. This orientation of the plate parts allowed the measurement of short transverse x- and long transverse y-component of elastic strains which are parallel to x and y principal axes. Coordinates of the gauge volume were kept constant in the short-transverse x- and longitudinal z-directions at 2.5 and 6.0 mm respectively and the gauge volume was expanded 4 mm along the longitudinal z-direction. The gauge volume is determined in a way to get an averaged state of long- and short-transversal strains along the longitudinal direction. So that, the length of the gauge volume along the longitudinal z-direction is determined to be 4 mm while other dimensions were kept at 2 mm. Measurements were performed at y-coordinates with 3 mm spacing from 0 to -15 mm and 5 mm spacing from -15 to -65 mm at a total of 16 point in both as-welded and heat-treated specimens along the long-transversal y-direction. Data from each bank (D1 and D2 as illustrated in Figure 2) are investigated separately to calculate short transverse x-component of strain using the data from D1 and long transverse y-component of strain using the data from D2. An example of TOF diffraction spectrum of Inconel alloy 740H obtained from a single bank is illustrated in Figure 3. The

https://doi.org/10.1016/j.mechmat.2020.103316

time of measurements were selected in a way to capture details about the fundamental reflections in the TOF diffraction spectrum.

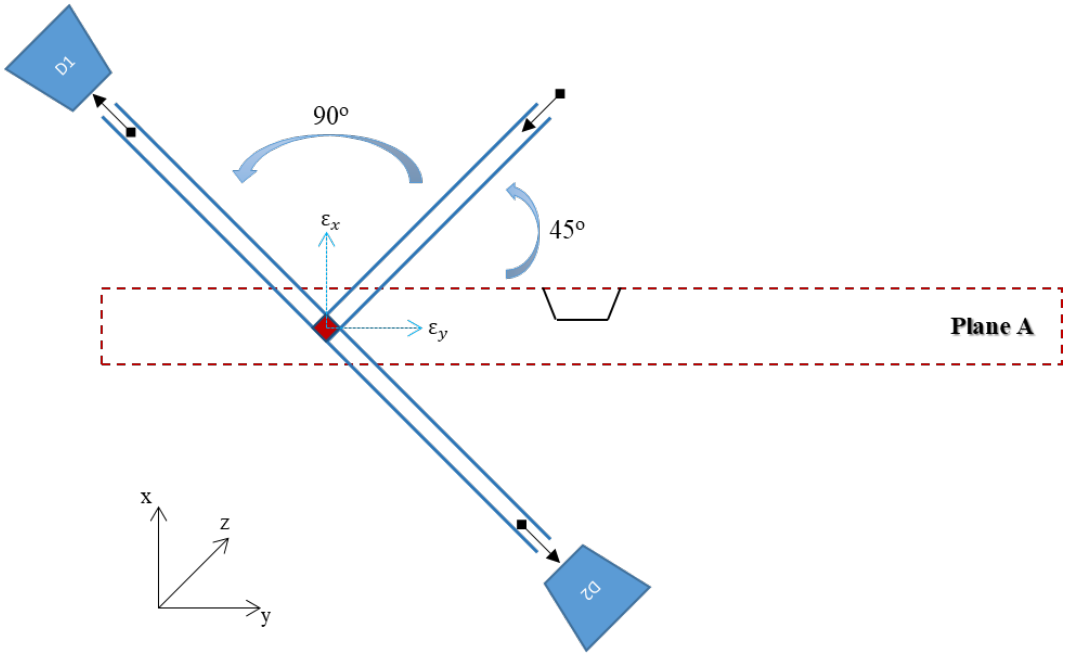


Figure 2. Schematic diagram of the time of flight neutron strain scanning of bead-on-plate Inconel alloy 740H specimens.

Nickel-based superalloys consist of an Al $\gamma$ matrix with a dispersion of $\gamma'$ precipitates that possess an ordered L12 structure. The diffraction pattern from the disordered FCC γ matrix produces fundamental reflections only, from planes with unmixed (all even or all odd) *hkl* indices, whereas the ordered $\gamma'$ precipitate phase produces both fundamental and superlattice reflections from planes with mixed *hkl* indices. For the strain analysis performed in this study the fundamental reflections {220}, {200} and {111} were used, which contain information for both γ and γ′ phases.

https://doi.org/10.1016/j.mechmat.2020.103316

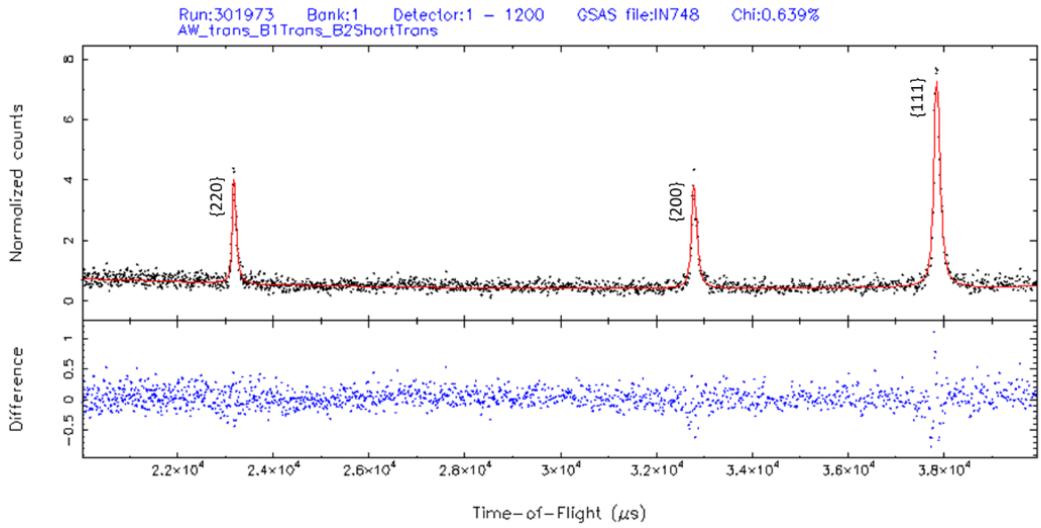


Figure 3. TOF diffraction spectrum of reference condition of Inconel alloy 740H obtained using ISIS ENGIN-X software, Open Genie.

ISIS ENGIN-X software, Open Genie, was used for the analysis of the neutron strain scanning data. After determination of the peak positions in the TOF diffraction spectrum by least-squares refinement process, Bragg's law was used to obtain d-spacing. The atomic inter-planar distance, $d$, were compared with the reference condition, $d_{ref}$, to calculate elastic strains, $\varepsilon_x$ and $\varepsilon_y$, using Equation 1. Preuss et al. (2002) previously reported the variations in the stress free lattice parameter in nickel based superalloys used for applications that operate under high temperature and pressure conditions. Similar to the Inconel alloy 740H, the superalloy investigated in that study had high $\gamma'$ precipitate phase. Results of that study shows that maximum variation of stress-free lattice parameter reaches up to 0.08 % in the heat-affected zone of the as-welded specimen while it is less than 0.01 % in the heat-treated condition. Accordingly, the chemical changes in the heat-affected zone has an influence on $d_{ref}$ in the as-welded condition while it does not cause a significant variation in the post-weld heat treated condition. The shift of $d_{ref}$ seems to be available only in a very narrow region of the heat-affected zone of the as-welded specimen and covers 2 mm in the axial direction. As

https://doi.org/10.1016/j.mechmat.2020.103316

the results of this study covers only a single measurement point at the core of the heat affected zone, a constant $d_{ref}$ is determined as the average of edge-of-plate measurements from all bottom corners of the as-welded specimen without extracting any part using the same gauge volume (Pratihar et al., 2009).

$$\varepsilon_{x,y} = \left(d - d_{ref}\right)/d_{ref} \quad (1)$$

There are various methods represented for the approximation of macroscopic elastic strains measurement using neutron strain scanning. One option is the determination of a weighted average of several single peak strains (Kamminga et al., 2000) and the other approximation method is using the change in the average lattice parameters (Daymond et al., 1997). In this study, neutron diffraction strains were approximated from all three different peak values in the TOF diffraction spectrum.

## 5. RESULTS

Neuron diffraction measurements were performed within one half of the plates along the transversal y-direction starting from the centre of the weld zone and strains were calculated as the mean of three different peak values for each measurement. Mean neutron diffraction strain values are represented within the range of standard error of mean. As neutron strain scanning results represent average strain within the gauge volume, results of the AI-eig contour method are determined as the mean of strains corresponding to 15 sampling points that take place in a volume with same geometric properties of the gauge volume. Figure 4 illustrates dimensions of the gauge volume and coordinates of the sampling points that are normalised to median of centre of the gauge volume.

https://doi.org/10.1016/j.mechmat.2020.103316

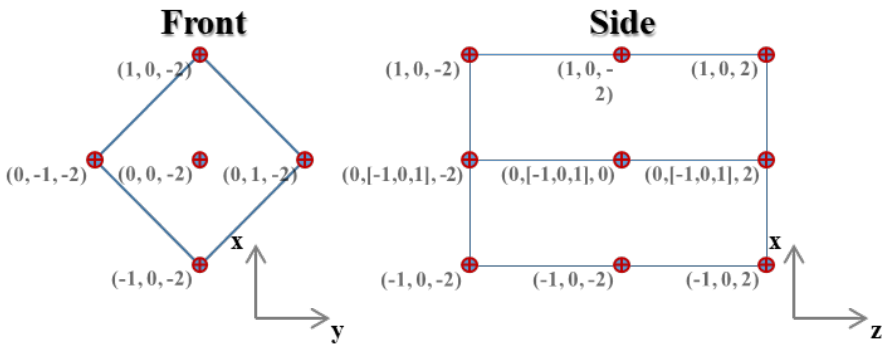


Figure 4. Front and side views of the gauge volume and data sampling points with normalised coordinates in millimetres (mm).

AI-eig contour method is able to reconstruct all components of residual strains after the determination of distribution of permanent plastic strains by the artificial agent. Using the same distribution of permanent plastic strains, it is also possible to reconstruct residual strains after the machining of a specimen if the machining process does not create additional permanent plastic strain fields. This property of eigenstrain theory was used for the reconstruction of residual strains after the EDM cut process which is assumed to create no eigenstrain field in addition to the fields formed as a result of welding process. Distribution of longitudinal z-component of residual strains before and after the EDM cut process are illustrated in Figure 5. This figure shows the residual strain relaxation and the change in distortion after the cutting process clearly. More detailed results about distortions in the same specimens can be found in the previous study of present authors (Uzun et al., 2018). For the purpose of validation of the AI-eig contour method, short transverse x- and long transverse y-components of residual strain in the as-welded and heat-treated specimens were measured after the EDM cut process.

https://doi.org/10.1016/j.mechmat.2020.103316

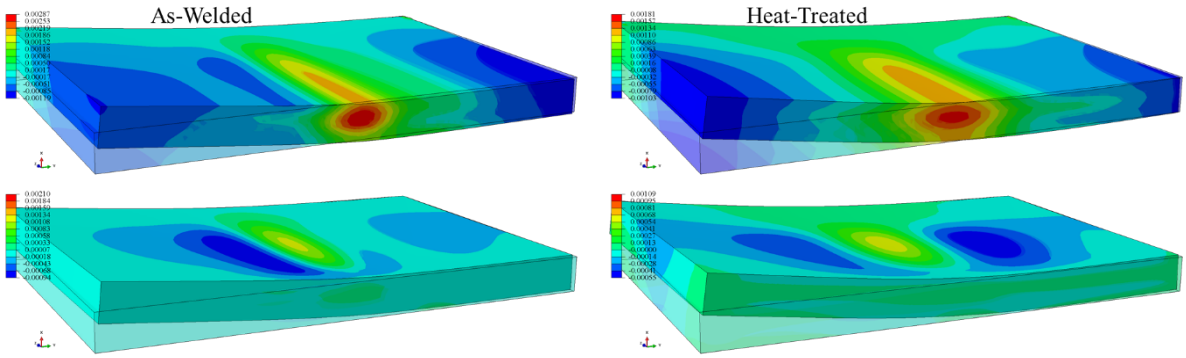


Figure 5. Distribution of longitudinal z-component of residual strains in the as-welded and heat-treated specimens and distortions, that are magnified with a factor of 10, before (top) and after (bottom) the cutting process. Validation is done using the after-cut state of specimens.

AI-eig contour method determines distribution of long transverse y- and longitudinal z-components of eigenstrains using experimental data of longitudinal z-component of out-of-plane displacements that are formed as a result of relaxation of longitudinal z-component of residual strains after the EDM cut process. This complex process could be achieved by the use of artificial agent (Uzun and Korsunsky, 2019a). The availability of the long transverse y-component of eigenstrains allows calculation of residual strains parallel to that component of eigenstrain and determination of weld distortions as illustrated in Figure 5. In this solution of AI-eig contour method, short transverse x-component of eigenstrains are assumed to have a minor effect on the formation of residual strains and they are neglected, but finite element solutions include calculations of all components of strains. The distribution of principal components of residual strains within the corresponding experimental gauge volumes after determination of the mean are given in Figure 6. Principal components of residual strains are compared in terms of absolute ratio with the longitudinal z-component of residual strains at the same measurement point. Results show that the magnitude of absolute ratio reaches to magnitudes, that are much higher than the Poisson's ratio of Inconel alloys which is 0.28, at different regions of the profile distribution in the y-direction. According to these results it can

be stated that the use of two components of eigenstrain with single component of experimental data in an artificial intelligence-based solution procedure, that assigns all model variables, allows the determination of complex distribution of all components of residual strain independent from Poisson's ratio.

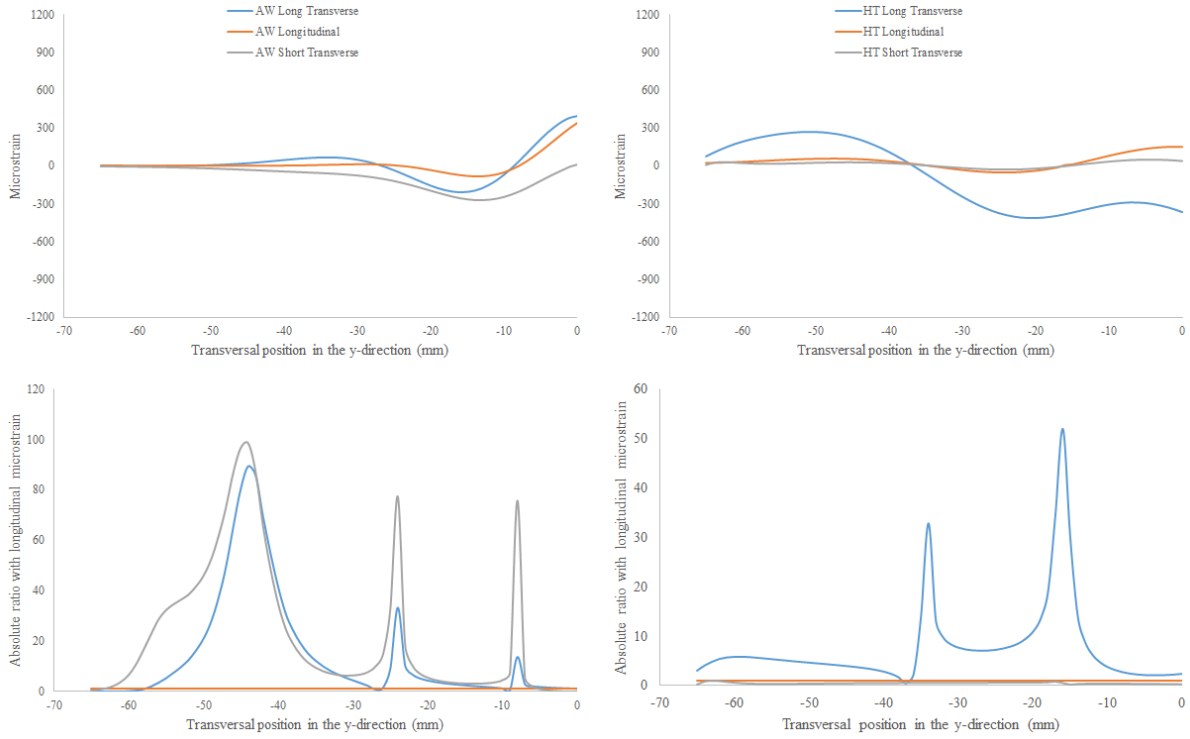


Figure 6. Mean values of sort transverse x-, long transverse y- and longitudinal z-components of microstrain in as-welded (AW) and heat-treated (HT) specimens in the gauge volume calculated by AI-eig contour method and their absolute ratio with longitudinal z-component of microstrain in each specimen.

As illustrated in Figure 6, the peaks of absolute ratio are at different positions with varying magnitudes in as-welded and heat-treated specimens. As it is expected, peak of magnitude of long transverse y- and longitudinal z-components of strain decreases after post-weld heat treatment (PWHT), but peak magnitude and distribution of long transverse y-component of strain changes completely. These results show that heat-treatment process replaces majority of

https://doi.org/10.1016/j.mechmat.2020.103316

elastic strains with permanent creep strains and reduces the peak magnitudes of absolute strain ratios but additional permanent creep strains cause formation of new strain fields at a lower magnitude. In the current solution, new strain fields seem to be formed after PWHT in the long transverse y-direction at a different magnitude and absolute ratio. It can be concluded that the conventional PWHT allows the relief of elastic strains to a limited extend. For additional information about the effect of PWHT conditions on the stress relief and creep strain formation can be found in the study of current authors (Uzun and Korsunsky, 2019b).

Residual strains in the specimens after the EDM cut of Inconel alloy 740H as results of calculations of the AI-eig contour method are given as mean values that range between the upper and lower boundaries of standard deviation. Rectangular shape of gauge volume allowed covering a wide range of the material that include high and low strain regions. As a result of having a rectangular gauge volume that extends in the longitudinal z-direction, mean values determined using the AI-eig contour method have high standard deviations at regions that are close to weld zone. Comparison of short and long transverse strains in the as welded and heat-treated specimens measured by the neutron strain scanning with the averaged calculations of the AI-eig contour method are illustrated in Figure 7. Results show that the AI-eig contour method have the same distribution of residual strains as the neutron strain scanning measurements, however magnitude of averages show slight deviation.

The proposed study is composed of several experimenting and modelling stages that could not be assigned to an artificial agent. The complexity of these stages can cause uncertainties. For minimizing the errors caused by through the thickness variation of the gauge volume, cross-section of the gauge volume is formed as a square with 2 mm side length which is half of its length as illustrated in Figures 2 and 4. The gauge volume is extended 4 mm along the

https://doi.org/10.1016/j.mechmat.2020.103316

longitudinal z-direction as illustrated in Figure 4 and neutron strain scanning measurements provided an average of strains within this volume. This average state is difficult to be mimicked using the simulation results. To get a similar state of strain averaging within the gauge volume, mean of the simulation results were calculated within an identical volume.

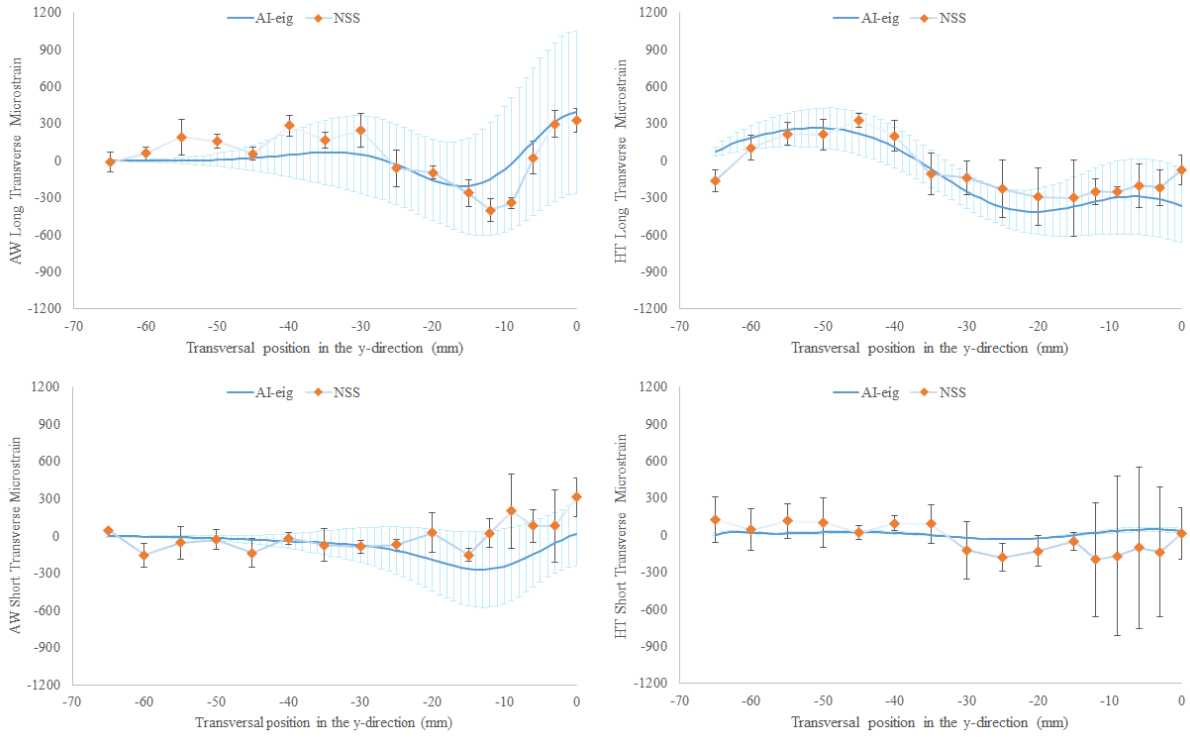


Figure 7. Long- and short-transverse strains in the as-welded and heat-treated specimens measured by the neutron strain scanning (NSS) method and calculated by the artificial intelligence based eigenstrain (AI-eig) contour method.

The AI-eig contour method calculations and the neutron strain scanning measurements were compared in terms of the results of the cut state of the specimens. The difficulties on modelling of the strain state after the relaxation of longitudinal z-component of residual strains at the cut edges and averaging within the gauge volume increased standard deviation in the model calculations. Although there are difficulties that have caused uncertainties, results show that range of results of the neutron strain scanning measurements and calculations of the

artificial intelligence-based eigenstrain contour method match at almost all measurement points. Averaged results of the experimental measurements and the model calculations have similar trends.

Maximum measurement error in a bank is 0.0139 percent of the lattice constant determined at the same measurement. This ratio is almost the same at each measurement point and is lower when compared to the errors from the approximation of macroscopic lattice constants. So that, they were not included in the elastic strain results. In this study, the approximation was done using TOF information corresponding to three different planes. This process resulted with errors relatively higher in and around the heat affected zone of the heat-treated specimen when compared to the other sections of the same specimen. The increasing influence of $\gamma'$ phase after the heat treatment process on (200) reflection, that consists of $\gamma$ and $\gamma'$ peaks, caused deviation on the TOF peaks that increased the uncertainty in the heat affected zone. The reason for having this kind of effect of $\gamma'$ is the differences in chemical composition formed in the heat affected zone during the welding process, but the mechanism behind formation of these differences should be further investigated.

## 6. DISCUSSION AND CONCLUSION

The contour method and its combination with eigenstrain theory provided new insights on the determination of strain and stress states of materials after complex manufacturing processes, but the eigenstrain contour method requires a complicated solution procedure that needs several trials to determine correct eigenstrain distribution. Based on the complexity of the problem, the number of trials could reach to hundreds. This laborious trial and error process can be performed for research and development purposes, but it is not a practical approach for

the industrial purposes. Accordingly, AI-eig contour method was developed by meeting principles of artificial intelligence with the eigenstrain contour method to deal with this difficulty. The proposed AI based method provided perfect match of simulation results with experimental contour method calculations in the prementioned studies performed in MBLEM. As being validated by diffraction techniques, the contour method provided the reliability of the AI-eig contour method, but its own validation by diffraction techniques was still missing. This study provided validation of the AI-eig contour method using the neutron diffraction technique at a complicated after-cut state. However, residual strains after different manufacturing processes should be investigated and validated using reliable experimental techniques like diffraction or FIB-DIC to be able to state that this method can be applied to industrial problems for the determination of residual strain and stress states.

The inverse problem of determining the underlying 3D eigenstrain distribution from a limited number of measurements of displacements (contour) or strains (FIB-DIC or diffraction) is ill-posed and/or ill-conditioned in the absence of some regularising assumptions.

In our previous publications (Uzun and Korsunsky, 2018, 2019a) the absence of transverse measurements was dealt with by introducing regularising assumptions, such as a fixed ratio between transverse and longitudinal eigenstrains. The transfer of this assumption from the context of shot-peening may be questioned from the viewpoint of *correctness*, but it delivers *uniqueness* to the solution, provided the ratio is fixed.

In the study devoted to the identification of main source of welding residual stress (Uzun, 2018), first single component (longitudinal only), and then multi-components solutions were

analysed to find the best match to experimental data. It was concluded that the eigenstrain domain may need to be adjusted by an intelligent operator.

In the next procedure, still in the absence of transverse measurements, an artificial agent was developed to deal with this task in an efficient way to determine parameters of multi-component solution (Uzun, 2019a).

In the present study transverse measurement of elastic strains by neutron diffraction was added. This 'tightens' the problem formulation considerably and allows one to release the value of the eigenstrain ratio as a refinable parameter. Once again, the linearity of eigenstrain formulation and least squares matching ensures both the existence and uniqueness of a solution. What makes the problem non-linear is the variable eigenstrain domain used in the formulation that is dealt with by the use of AI agent.

The systematic minimisation search that is used ensures finding a **global minimum** of the sum-of-squares mismatch function. This corresponds to the best approximate solution of the regularised problem, as posed by the authors. By virtue of using eigenstrain formulation, this solution satisfies the mechanics constraints (stress equilibrium, strain compatibility, boundary conditions).

The artificial intelligence based eigenstrain contour method have successfully reconstructed residual strains using only a single component of displacement data. The quality and high sensitivity of out-of-plane deformations, obtained using coordinate measuring machine, allowed determination of all components of residual strains. Results of neutron strain scanning on the short transverse x- and long transverse y-components of residual strain

showed that calculations of the eigenstrain methods have good agreement with experimental measurements in terms of distribution. Although, there are minor differences between the magnitudes of averaged model and experiment results, it can be stated that the artificial intelligence based eigenstrain contour method is capable of determination distribution of all components of principal strains with a similar trend of highly reliable experimental measurement technique.

## ACKNOWLEDGEMENTS

The Scientific and Technological Research Council of Turkey (TUBITAK) supported this study through grant Number: TUBITAK- BIDEB-2219. European Commission Research Executive Agency (REA) supported this research through grant MSCA-IF no. 794957 (RESTREIG). AMK acknowledges EPSRC funding, including through grants EP/S005072 and EP/I020691. The authors would like to thank Dr Steve McCoy of Special Metals Corporation for providing Inconel alloy 740H specimens.

## REFERENCES

Ahn, J., He, E., Chen, L., Wimpory, R.C., Dear, J.P., Davies, C.M., 2017. Prediction and measurement of residual stresses and distortions in fibre laser welded Ti-6Al-4V considering phase transformation. Mater. Des. 115, 441–457. https://doi.org/10.1016/j.matdes.2016.11.078

Allen, A.J., Hutchings, M.T., Windsor, C.G., Andreani, C., 1985. Neutron diffraction methods for the study of residual stress fields. Adv. Phys. 34, 445–473.

https://doi.org/10.1016/j.mechmat.2020.103316

https://doi.org/10.1080/00018738500101791

Blunden, J., Arndt, D.S., 2019. A Look at 2018 Takeaway Points from the State of the Climate Supplement. Bull. Am. Meteorol. Soc. 1527–1538. https://doi.org/10.1175/BAMS-D-19-0193.1

Brown, D.W., Holden, T.M., Clausen, B., Prime, M.B., Sisneros, T.A., Swenson, H., Vaja, J., 2011. Critical comparison of two independent measurements of residual stress in an electron-beam welded uranium cylinder: Neutron diffraction and the contour method. Acta Mater. 59, 864–873. https://doi.org/10.1016/j.actamat.2010.09.022

Daymond, M. ~R., Bourke, M. ~A. ~M., Von Dreele, R. ~B., Clausen, B., Lorentzen, T., 1997. Use of Rietveld refinement for elastic macrostrain determination and for evaluation of plastic strain history from diffraction spectra. J. Appl. Phys. 82, 1554–1562. https://doi.org/10.1063/1.365956

DeWald, A.T., Hill, M.R., 2006. Multi-Axial Contour Method for Mapping Residual Stresses in Continuously Processed Bodies. Exp. Mech. 46, 473–490. https://doi.org/10.1007/s11340-006-8446-5

Everaerts, J., Salvati, E., Uzun, F., Romano Brandt, L., Zhang, H., Korsunsky, A.M., 2018. Separating macro- (Type I) and micro- (Type II+III) residual stresses by ring-core FIB-DIC milling and eigenstrain modelling of a plastically bent titanium alloy bar. Acta Mater. 156, 43–51. https://doi.org/10.1016/j.actamat.2018.06.035

Gianfrancesco, A. Di, 2017. Materials for Ultra-Supercritical and Advanced Ultra-Supercritical Power Plants. Elsevier Ltd. https://doi.org/https://doi.org/10.1016/B978-0-08-100552-1.00001-4

Johnson, M.W., Edwards, L., Withers, P.J., 1997. Engin - A new instrument for engineers. Phys. B Condens. Matter 234–236, 1141–1143. https://doi.org/10.1016/S0921-4526(97)89272-1

https://doi.org/10.1016/j.mechmat.2020.103316

Kamminga, J.-D., de Keijser, T.H., Mittemeijer, E.J., Delhez, R., 2000. New methods for diffraction stress measurement: a critical evaluation of new and existing methods. J. Appl. Crystallogr. 33, 1059–1066. https://doi.org/10.1107/s0021889800004258

Kartal, M., Turski, M., Johnson, G., Fitzpatrick, M.E., Gungor, S., Withers, P.J., Edwards, L., 2006. Residual stress measurements in single and multi-pass groove weld specimens using neutron diffraction and the contour method. Mater. Sci. Forum 524–525, 671–676. https://doi.org/10.4028/www.scientific.net/MSF.524-525.671

Kartal, M.E., Kang, Y.H., Korsunsky, A.M., Cocks, A.C.F.F., Bouchard, J.P., 2016. The influence of welding procedure and plate geometry on residual stresses in thick components. Int. J. Solids Struct. 80, 420–429. https://doi.org/10.1016/j.ijsolstr.2015.10.001

Kelleher, J., Prime, M.B., Buttle, D., Mummery, P.M., Webster, P.J., Shackleton, J., Withers, P.J., 2003. The Measurement of Residual Stress in Railway Rails by Diffraction and other Methods. J. Neutron Res. 11, 187–193. https://doi.org/10.1080/10238160410001726602

Korsunsky, A.M., 2017. A Teaching Essay on Residual Stresses and Eigenstrains. Butterworth-Heinemann, 212p. https://www.sciencedirect.com/science/book/9780128109908

Pang, W.K., 2014. Understanding and improving the thermal stability of layered ternary carbides in ceramic matrix composites. Adv. Ceram. Matrix Compos. 340–368. https://doi.org/10.1533/9780857098825.2.340

Pratihar, S., Turski, M., Edwards, L., Bouchard, P.J., 2009. Neutron diffraction residual stress measurements in a 316L stainless steel bead-on-plate weld specimen. Int. J. Press. Vessel. Pip. 86, 13–19. https://doi.org/10.1016/j.ijpvp.2008.11.010

Preuss, M., Pang, J.W.L., Withers, P.J., Baxter, G.J., 2002. Inertia welding nickel-based

superalloy: Part II. Residual stress characterization. Metall. Mater. Trans. A Phys. Metall. Mater. Sci. 33, 3227–3234. https://doi.org/10.1007/s11661-002-0308-x

Prime, M.B., 1999. Measuring residual stress and the resulting stress intensity factor in compact tension specimens. Fatigue Fract. Eng. Mater. Struct. 22, 195–204. https://doi.org/10.1046/j.1460-2695.1999.00155.x

Prime, M.B., Hughes, D.J.D.J., Webster, P.J.P.J., 2001. Weld application of a new method for cross-sectional residual stress mapping. Soc. Engineeering Mech. Annu. Conf. Expo. 836, 1–5.

Rangaswamy, P., Griffith, M.L., Prime, M.B., Holden, T.M., Rogge, R.B., Edwards, J.M., Sebring, R.J., 2005. Residual stresses in LENS® components using neutron diffraction and contour method. Mater. Sci. Eng. A 399, 72–83. https://doi.org/10.1016/j.msea.2005.02.019

Ritchie, H., Roser, M., 2019. Fossil Fuels. Our World Data.

Santisteban, J.R., Daymond, M.R., James, J.A., Edwards, L., 2006. ENGIN-X: A third-generation neutron strain scanner. J. Appl. Crystallogr. 39, 812–825. https://doi.org/10.1107/S0021889806042245

Shokrieh, M.M., Ghanei Mohammadi, A.R., 2014. Non-destructive testing (NDT) techniques in the measurement of residual stresses in composite materials: an overview. Residual Stress. Compos. Mater. 58–75. https://doi.org/10.1533/9780857098597.1.58

Smith, M.C., Smith, A.C., Ohms, C., Wimpory, R.C., 2018. The NeT Task Group 4 residual stress measurement and analysis round robin T on a three-pass slot-welded plate specimen. Int. J. Press. Vessel. Pip. 164, 3–21. https://doi.org/10.1016/j.ijpvp.2017.09.003

U.S. Energy Information Agency, 2013. International Energy Outlook 2013.

Uzun, F., Bilge, A.N., 2015. Ultrasonic Investigation of the Effect of Carbon Content in

Carbon Steels on Bulk Residual Stress. J. Nondestruct. Eval. 34. https://doi.org/10.1007/s10921-015-0284-x

Uzun, F., Everaerts, J., Brandt, L.R., Kartal, M., Salvati, E., Korsunsky, A.M., 2018. The inclusion of short-transverse displacements in the eigenstrain reconstruction of residual stress and distortion in in740h weldments. J. Manuf. Process. 36, 601–612. https://doi.org/10.1016/j.jmapro.2018.10.047

Uzun, F., Korsunsky, A.M., 2019a. On the application of principles of artificial intelligence for eigenstrain reconstruction of volumetric residual stresses in non-uniform Inconel alloy 740H weldments. Finite Elem. Anal. Des. 155, 43–51. https://doi.org/10.1016/j.finel.2018.11.004

Uzun, F., Korsunsky, A.M., 2019b. On the analysis of post weld heat treatment residual stress relaxation in Inconel alloy 740H by combining the principles of artificial intelligence with the eigenstrain theory. Mater. Sci. Eng. A 752, 180–191. https://doi.org/10.1016/j.finel.2018.11.004

Uzun, F., Korsunsky, A.M., 2018. On the identification of eigenstrain sources of welding residual stress in bead-on-plate inconel 740H specimens. Int. J. Mech. Sci. 145, 231–245. https://doi.org/doi.org/10.1016/j.ijmecsci.2018.07.007

Woo, W., An, G.B., Kingston, E.J., Dewald, A.T., Smith, D.J., Hill, M.R., 2013. Through-thickness distributions of residual stresses in two extreme heat-input thick welds: A neutron diffraction, contour method and deep hole drilling study. Acta Mater. 61, 3564–3574. https://doi.org/10.1016/j.actamat.2013.02.034

Zhang, Y., Ganguly, S., Stelmukh, V., Fitzpatrick, M.E., Edwards, L., 2003. Validation of the Contour Method of Residual Stress Measurement in a MIG 2024 Weld by Neutron and Synchrotron X-ray Diffraction. J. Neutron Res. 11, 181–185. https://doi.org/10.1080/10238160410001726594